Flat Fresnel doublets made of PMMA and PC: combining low cost production and very high concentration ratio for CPV

Fabian Languy,[1,*] Karl Fleury,[2] Cédric Lenaerts,[2] Jérôme Loicq,[2] Donat Regaert,[3] Tanguy Thibert,[2] and Serge Habraken[1]

[1]*Hololab, Physics Department, Bat. B5a, Université de Liège, 17 allée du 6 Août, B-4000 Liège, Belgium*
[2]*Centre Spatial de Liège, Avenue du Pré-Aily, B-4031 Angleur, Belgium*
[3]*Laboratoire de Physique du Solide, Facultés Universitaires Notre-Dame de la Paix, 61 rue de Bruxelles, B-5000 Namur, Belgium*
*flanguy@ulg.ac.be

Abstract: The linear chromatic aberration (LCA) of several combinations of polycarbonates (PCs) and poly (methyl methacrylates) (PMMAs) as singlet, hybrid (refractive/diffractive) lenses and doublets operating with wavelengths between 380 and 1600 nm – corresponding to a typical zone of interest of concentrated photovoltaics (CPV) – are compared. Those comparisons show that the maximum theoretical concentration factor for singlets is limited to about $1000 \times$ at normal incidence and that hybrid lenses and refractive doublets present a smaller LCA increasing the concentration factor up to $5000 \times$ and 2×10^6 respectively. A new achromatization equation more useful than the Abbé equation is also presented. Finally we determined the ideal position of the focal point as a function of the LCA and the geometric concentration which maximizes the flux on the solar cell.

OCIS codes: (080.4298) Nonimaging optics; (220.1770) Concentrators; (050.1965) Diffractive lenses; (220.1000) Aberration compensation; (160.4760) Optical properties.

References and links

1. C. Algora, "Very high concentration challenges of III–V multijunction solar cells," in *Concentrator Photovoltaics,* A. Luque, and V. Andreev, ed. (Springer, 2007), Chap. 5.
2. Spectrolab datasheet: *www.spectrolab.com/DataSheets/PV/CPV/CDO-100-C3MJ.pdf*, accessed on 02/06/2011.
3. Website for NREL's AM1, 5 Standard Data set: http://rredc.nrel.gov/solar/spectra/am1.5/ASTMG173/ASTMG173.html, accessed on 02/06/2011.
4. R. Winston, "Light Collection within the Framework of Geometrical Optics," J. Opt. Soc. Am. **60**(2), 245–247 (1970).
5. S. Puliaev, J. L. Penna, E. G. Jilinski, and A. H. Andrei, "Solar diameter observations at Observatório Nacional in 1998-1999," Astron. Astrophys. Suppl. Ser. **143**(2), 265–267 (2000).
6. J. Chaves, *Introduction to nonimaging optics* (CRC Press, 2008), Chap. 1.
7. E. Hecht, *Optics* 4th Ed. (Addison-Wesley, 2002), Chap. 5.
8. D. A. Buralli, G. M. Morris, and J. R. Rogers, "Optical performance of holographic kinoforms," Appl. Opt. **28**(5), 976–983 (1989).
9. Fresnel lens brochure of the Fresnel Technologies Inc.: *www.fresneltech.com/materials.html*, accessed on 02/06/2011.
10. S. N. Kasarova, N. G. Sultanova, C. D. Ivanov, and I. D. Nikolov, "Analysis of the dispersion of optical plastic materials," Opt. Mater. **29**(11), 1481–1490 (2007).
11. J. D. Lytle, "Polymeric Optics," in *Handbook of Optics*, 3rd Edition, Vol. IV, M. Bass, ed. (McGraw-Hill, 2009), Chap. 3.
12. ASAP™ optical design software of Breault Research Organization, *http://www.breault.com*.
13. Y. B. Lee, and T. H. Kwon, "Modeling and numerical simulation of residual stresses and birefringence in injection molded center-gated disks," J. Mater. Process. Technol. **111**(1-3), 214–218 (2001).
14. V. Moreno, J. F. Román, and J. R. Salgueiro, "High efficiency diffractive lenses: Deduction of kinoform profile," Am. J. Phys. **65**(6), 556–562 (1997).

15. D. C. O'Shea, T. J. Suleski, A. D. Kathman, and D. W. Prather, *Diffractive Optics: Design, Fabrication, and Test* (Spie Press, 2004), Chap. 4.
16. B. H. Kleemann, M. Seeßelberg, and J. Ruoff, "Design concepts for broadband high–efficiency DOEs," J. Eur. Opt. Soc. Rapid Publ. **3**, 08015 (2008).
17. F. Languy, C. Lenaerts, J. Loicq, and S. Habraken, "Achromatization of solar concentrator thanks to diffractive optics," presented at the 2nd Int'l Workshop on Concentrating Photovoltaic Power Plants, Darmstadt, Germany, 9–10 March 2009, *http://www.concentrating-pv.org/darmstadt2009/index.html*.
18. M. Born, and E. Wolf, *Principles of Optics*, 7th Ed. (Cambridge University Press, 2003), p. 188.
19. G. K. Skinner, "Design and imaging performance of achromatic diffractive-refractive x-ray and gamma-ray Fresnel lenses," Appl. Opt. **43**(25), 4845–4853 (2004).

1. Introduction

Nowadays, lots of optical systems like cameras, telescopes, microscopes etc. use an achromatic doublet of glasses, which delivers good image quality but is quite expensive, bulky and heavy. Even for a single glass lens the cost, bulk and weight might be a problem. This is why Fresnel lenses are often used, especially when built in optical plastic, e. g. headlights, solar concentrators, projectors, traffic lights, etc. So, in order to combine small chromatic aberrations with low-cost production, we suggest using achromatic Fresnel doublets for concentrated photovoltaics (CPV). The reduction of the chromatic aberration allows for a higher concentration ratio and a higher efficiency of multijunction photovoltaic cells [1]. Even if most optical systems work in the visible range, we extended our study to a typical zone of interest of wavelengths for solar concentration: from 380 to 1600 nm. Typically, out of this range the external quantum efficiency of a triple junction cell drops to about 40% [2] and the direct solar flux is also low [3].

2. Influence of the LCA on the optical concentration ratio

Considering a concentrator with a collector surface *A'* and a receiver surface *A*. The ratio *A'*/*A* corresponds to the geometrical concentration factor C_{geo}. If Φ' is the flux collected and Φ the flux absorbed, then Φ'/Φ refers to the optical efficiency η_{opt}. Finally, the optical concentration factor C_{opt} is given by Eq. (1).

$$C_{opt} = \eta_{opt} C_{geo} = \frac{\Phi'}{\Phi} \frac{A'}{A}. \tag{1}$$

For a collector of rotational symmetry, the upper limit of concentration is achieved with an optical efficiency of 100% and for a concentrator where both collector and absorber are immersed in the air is given by Eq. (2) where θ represents the acceptance half angle of the incoming light [4].

$$C_{opt}^{max} = \sin^{-2}\theta. \tag{2}$$

On Earth, for two degrees of concentration, the upper limit of solar concentration is about 46,000 due to an acceptance angle of the sun of ~960" (i.e. 0.267°) [5]. For a polychromatic source, this concentration may be achieved with reflective surfaces (like the compound parabolic concentrator [6]). But systems suffering from chromatic aberration will not be able to achieve such high concentration ratio. This is the case for lenses since their focal distances depend on the wavelength: $f = f(\lambda)$.

Considering two wavelengths λ_A and λ_B, the linear chromatic aberration (LCA) corresponds to the difference of the focal distances:

$$LCA = f(\lambda_B) - f(\lambda_A). \tag{3}$$

The way the focal distance of an ideal (with only chromatic aberration) thin refractive lens having a front and back radii of curvature R_1 and R_2 changes is given by Eq. (4) [7] while for a diffractive lens it is given by Eq. (5) [8].

$$\frac{1}{f_{ref}(\lambda)} \simeq \left(\frac{1}{R_1} - \frac{1}{R_2}\right)(n(\lambda) - 1), \tag{4}$$

$$f_{dif}(\lambda) = \frac{\lambda_A}{\lambda} f(\lambda_A). \tag{5}$$

Hereafter, we arbitrarily chose to take λ_0 as a reference: λ_0 is such that the minimum LCA and the maximum LCA – achieved with λ_m and λ_M respectively – are equal in absolute value. The system is thus optimised to decrease the maximum longitudinal chromatic aberration in absolute value $|LCA_{max}|$ (see Fig. 1a).
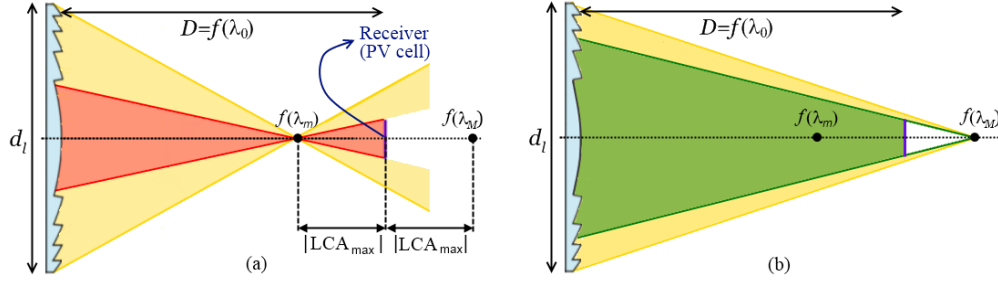

Fig. 1. Representation of the optical efficiency of two wavelengths having the same LCA in absolute value but having different optical efficiency (yellow part corresponds to losses).

For easier comparison, the notation with an asterisk as exponent is introduced, corresponding to a normalisation with λ_0. The LCA for the refractive and diffractive cases may be thus rewritten respectively as Eq. (6) and Eq. (7). It appears that both depend only on the wavelength. And it can be easily shown, that if the detector is placed in $f(\lambda_0)$, the geometrical concentration allowing for the collection of the whole flux is given by Eq. (8).

$$LCA_{ref}^*(\lambda) = \frac{f(\lambda) - f(\lambda_0)}{f(\lambda_0)} = \frac{n(\lambda_0) - n(\lambda)}{n(\lambda) - 1}, \tag{6}$$

$$LCA_{dif}^*(\lambda) = \frac{f(\lambda) - f(\lambda_0)}{f(\lambda_0)} = \left(\frac{\lambda_0}{\lambda} - 1\right), \tag{7}$$

$$C_{geo}^{max} = \left(\frac{1 - LCA^*}{LCA^*}\right)^2. \tag{8}$$

Imaging optics tends to decrease the $|LCA_{max}|$ but in non-imaging optics, to maximize the amount of collected rays on the collector, minimising the LCA is not sufficient. Figure 1 shows two wavelengths with the same LCA in absolute value but the amount of light collected with λ_m (red part) in Fig. 1a is more important than the amount of light collected with λ_M (green part) in Fig. 1b. It is easy to show that the ideal position of the detector z_{det} as a function of the LCA^* corresponds to a parabola of Eq. (30) (see Appendix A). This position allows for higher concentration as represented in Fig. 2a while Fig. 2b shows the gain of geometric concentration factor achieved by moving the detector from $f(\lambda_0)$ to z_{det}. In CPV, the maximum concentration is given by the angular size of the sun, but if the LCA^* is greater than 0.466% then the upper limit is driven by the LCA and becomes lower than 46,000.
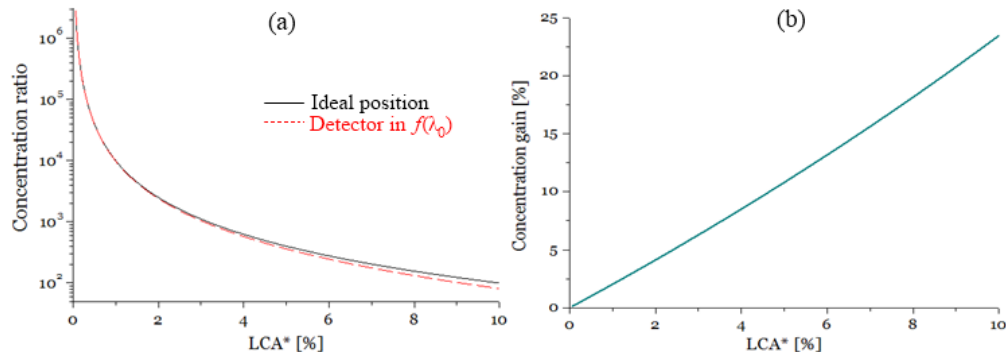
Fig. 2. Concentration ratio at normal incidence as a function of the LCA^* (a) and gain if the detector is moved from the position of the minimum $|LCA_{max}|$ to the ideal position (b).

However lens designers do not always have the choice of detector size and position. For a given $|LCA_{max}|$ and geometrical concentration factor, where should λ_0 be focused: before collector position or after? Focusing after the detector increases the LCA but the view angle of fast converging wavelengths decreases, which is favourable for systems with fast converging wavelengths with $\eta_{opt} < 1$. Focusing before the detector position decreases the LCA but a higher amount of fast converging wavelengths will miss the detector. The ideal position and the optical efficiency as a function of the LCA^* and the geometrical concentration factor are given in Fig. 3.
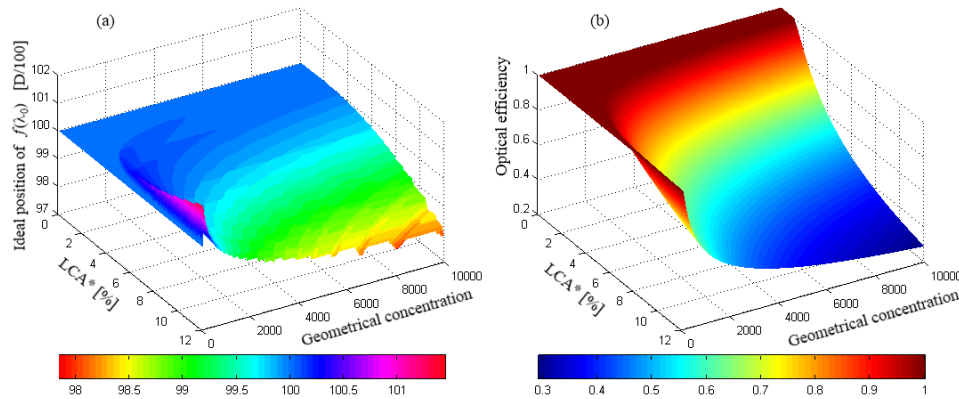

Fig. 3. Ideal position of $f(\lambda_0)$ (a) and optical efficiency (b) as functions of the LCA^* and the geometrical concentration.

A very important point of this section is that the optical concentration factor could be even more limited by the LCA rather than by the acceptance angle.

3. Dispersion curves

PMMA is probably the most common optical plastic (OP) used in solar concentration thanks to its high transmittance and low dispersion curve. Another common OP used for Fresnel lenses is PC, with similar spectral transmission and high impact resistance [9]. Thanks to their high difference of refractive index (about 0.1 at 550 nm), PC and PMMA are good candidates for refractive doublets. Some data about OPs may be found in Kasarova *et al.* article [10], Handbook of optical materials [11] and some ray tracing software like ASAP[TM] [12]. But depending on the supplier and the injection parameters, OPs properties change. This is why we made our own ellipsometric measurements on several samples. Eight OPs were taken, three from the literature and we determined the dispersion curve of five OPs coming from our suppliers. In total five PCs and five PMMAs listed in Table 1 were studied.

Table 1. Information about the PMMAs and PCs

PMMA	Data	Provider (P) or Trade Mark (TM)	PC	Data	Provider (P) or Trade Mark (TM)
PMMA #1	[11]	Unknown	PC #1	[10][1]	Unknown
PMMA #2	CSL[2]	Altuglas (TM)	PC #2	[11]	Unknown
PMMA #3	CSL[2]	Diakon (TM)	PC #3	CSL[2]	Calibre 1080 DVD (TM)
PMMA #4	CSL[2]	Evonik (P)	PC #4	CSL[2]	Makrolon (TM)

[1] Referenced as PC in [10].
[2] CSL: Ellipsometric measurements from Centre Spatial of Liege

The refractive index n depends on the wavelength λ. The way the refractive index changes with the wavelength might be approximated with several functions. Two popular functions of dispersion are used in this publication. Equation (9) corresponds to Sellmeier's equation and Eq. (10) to Laurent's (also called Schott's) equation. In this article, Sellmeier's equation is limited to $m = 3$ and Laurent's equation is limited to the term in λ^{-8} ensuring typically a difference lower than ± 0.001 between interpolated and experimental data [10].

$$n(\lambda) = \sqrt{1 + \sum_{i=1}^{m} \frac{B_i \lambda^2}{\lambda^2 - C_i}}, \tag{9}$$

$$n(\lambda) = \sqrt{A_1 + A_2 \lambda^2 + \frac{A_3}{\lambda^2} + \frac{A_4}{\lambda^4} + \frac{A_5}{\lambda^6} + \cdots}. \tag{10}$$

The dispersion coefficients are presented in Table 2. Note that those coefficients must be used with the wavelength expressed in microns, both Laurent's and Sellmeier's equations were used for each sample, but only the one giving the smallest is presented. The curves of the refractive indexes are presented in Fig. 4 (a) and (b) for PMMAs and PCs respectively. The variation of refractive index from a sample to another might be explained by the fact that industrial process is not constant and injection parameters might be different for every injection leading to variation in the refractive index [13]. Nevertheless, the curve "PC #1 (old)" has an abnormal behaviour: above 1200 nm the refractive index drops too rapidly compared to any other PCs. This might be simply explained by the fact that the dispersion coefficients were retrieved by Kasarova *et al.* from measurements going from 435.8 to 1052 nm and the extrapolation outside of this range gives wrong results. We performed another interpolation (PC #1) giving more probable results in the near infrared region. Thus, PC #1 (old) will no longer be considered hereafter.
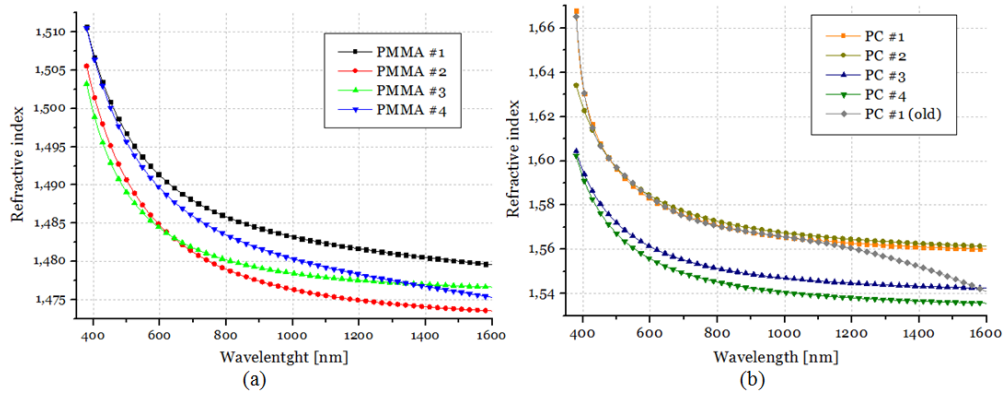

Fig. 4. Dispersion curves of PMMAs (a) and PCs (b).

Table 2. Dispersion coefficients some PCs and PMMAs

Material	Dispersion coefficients					
(L/S)[1]	A_1 or B_1	A_2 or C_1	A_3 or B_2	A_4 or C_2	A_5 or B_3	A_6 or C_3
PMMA #1 (L)	2.190664	-2.330317e-3	1.122194e-2	4.765210e-4	-5.040529e-5	3.423433e-6
PMMA #2 (S)	4.841120e-1	3.353637e-4	6.815579e-1	1.096254e-2	1.028035e-2	1.184708e-2
PMMA #3 (S)	6.997099e-1	2.731275e-1	2.043425e-1	-5.777416e-4	-5.784644e-4	4.291190e-2
PMMA #4 (S)	1.838458e-1	2.827502e+1	0. 998312e-1	1.127337e-2	6.664339e+3	1.127703e-2
PC #1 (S)[2]	1.341659e-2	2.410966e-1	1.168465e+0	1.329927e-1	1.811373e-2	1.812526e-2
PC #2 (L)	2.430734e+0	-1.343233e-3	2.714995e-2	3.244405e-4	7.013408e-5	5.615956e-6
PC #3 (S)	2.583939e-2	3.675250e-1	9.769463e-1	9.453662e-2	1.4831288e-2	1.488111e-2
PC #4 (S)	2.205583e-2	2.532511e-1	1.073656e+0	1.004816e-1	1.630428e-2	1. 623521e-2

[1] Dispersion mode: Laurent (L) or Sellmeier (S)

[2] Recalculated dispersion coefficients to get more probable results in the near infrared region

4. Chromatic aberration of single lenses

4.1 Refractive lens

For an ideal (with only chromatic aberration) thin refractive lens in paraxial condition, the focal distance f may be approximated by Eq. (4) which has been rewritten in Eq. (11):

$$f(\lambda) \simeq \frac{RoC_{eq}}{n(\lambda)-1},\qquad(11)$$

with RoC_{eq} the equivalent radius of curvature of the lens [7]. Following the definition of the asterisk as an exponent

$$RoC_{eq}^{*} = \frac{RoC_{eq}}{f(\lambda_0)} = \left(\frac{R_1 R_2}{R_2 - R_1}\right)\frac{1}{f(\lambda_0)} = (n(\lambda)-1)\times100\%.\qquad(12)$$

As explain in the previous section, the system is optimised to decrease the maximum longitudinal chromatic aberration in absolute value $|LCA_{max}|$ giving the focal distances of Fig. 5.
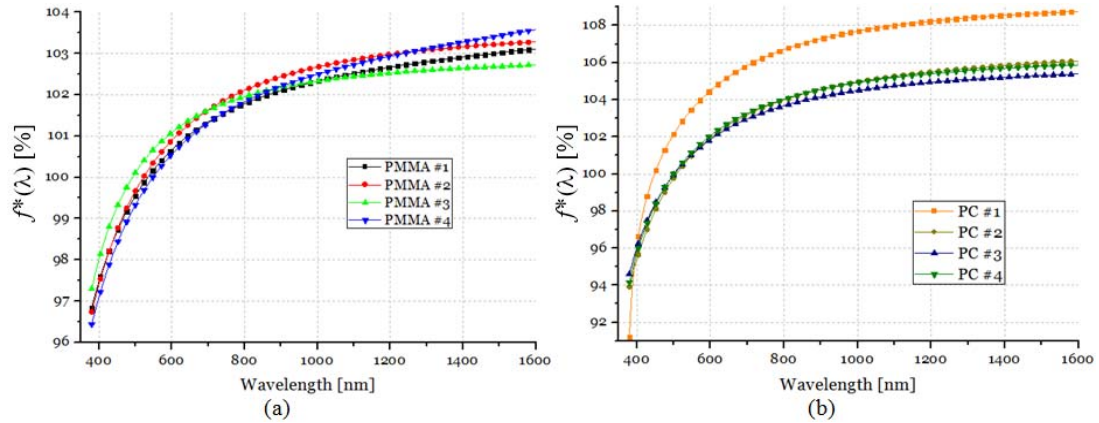

Fig. 5. Relative focal distances for PMMAs (a) and PCs (b).

Table 3 hereunder gives the central wavelength (λ_0) and compares the $|LCA^{*}_{max}|$ of each material as well as the equivalent radius of curvature. In the case of a singlet, $|LCA_{max}|$ is achieved for the two extreme wavelengths: $\lambda_m = 380$ nm and $\lambda_M = 1600$ nm. As shown on Fig. 4 and 5, the LCA is more important for PCs than PMMAs. This is due to the high dispersion of the refractive indexes of PCs compared to the refractive indexes of PMMAs. It is common to use the Abbé number v_d to measure the dispersion in the visible region.

$$v_d = (n_d - 1)/(n_F - n_C), \tag{13}$$

d, F and C being three Fraunhofer lines in the visible region corresponding respectively to 587.562, 486.134 and 656.281 nm. In order to take into account the wide spectrum band studied, we use the solar Abbé number $v_\odot$:

$$v_\odot = (n_{990nm} - 1)/(n_{380nm} - n_{1600nm}). \tag{14}$$

Table 3. Data for Singlets

Material	Information for singlets					
	λ_0 [nm]	RoC_{eq}^* [%]	LCA^* [%]	C_{opt}^{max}	v_d	$v_\odot$
PMMA #1	534	48.995	3.159	1002	57.231	15.561
PMMA #2	522	48.906	3.282	928	52.270	14.868
PMMA #3	492	48.959	2.720	1351	66.522	17.990
PMMA #4	548	49.231	3.579	781	51.710	13.642
PC #1	448	60.911	8.794	129	27.928	5.249
PC #2	508	59.556	6.086	270	29.894	7.806
PC #3	502	57.166	5.393	344	33.746	8.854
PC #4	500	56.717	5.877	290	33.271	8.106

4.2 Diffractive lens

Diffractive lenses may be designed in different ways. For a single wavelength, only the kinoform (Fig. 6) may have one focus and a theoretical diffraction efficiency of 100% [14]. The ideal kinoform looks like a Fresnel lens, composed of a multitude of zones with a constant thickness h of few microns. Each zone of the diffractive lens is designed by keeping the optical path length constant all over the zone. Between two adjacent zones, a 2π-phase shift is introduced. In other words, there is no discontinuity in the wavefront and the diffraction efficiency is maximum at the designed wavelength λ_0. This continuity is ensured by a constant thickness of the teeth: $h = \lambda_0 / (n(\lambda_0) - 1)$ [8].
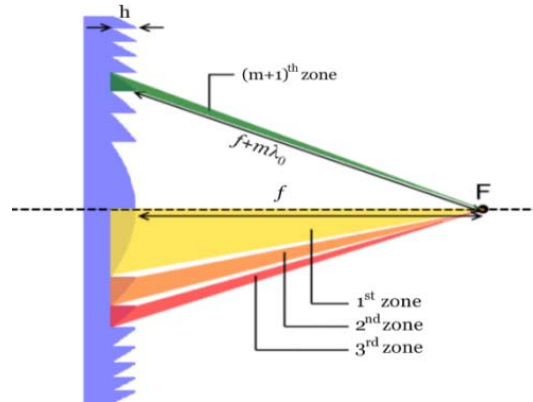

Fig. 6. Schematic representation of a kinoform diffractive lens.

While illuminating the lens with another wavelength, the focal distance will be modified following Eq. (5), independently of the refractive index . The Abbé number corresponding to this dispersion is thus also independent of the refractive index [15] and is given by Eq. (15).

$$v_{d,diff} = \frac{d}{F - C} = -3.4518. \tag{15}$$

Similarly, $v_\odot = -0.8115$. The Abbé number is negative and has lower absolute value than any refractive material, meaning that for a converging lens, long wavelengths will converge

shorter than short wavelengths and that diffractive lenses are more dispersive which is unfavourable for small *LCA* designs. Moreover, the farther they are used from the design wavelength, the more diffractive lenses suffer from a lack of diffraction efficiency. The diffraction efficiency at the first order η_1 is given by Eq. (16). E. g., for PMMA #2, with $\lambda_0 = 550$nm, the diffraction efficiency at the first order remains above 90% only between 472 and 663 nm.

$$\eta_1(\lambda) = \text{sinc}^2 \left\{ 1 - \frac{\lambda_0}{\lambda} \frac{n(\lambda)-1}{n(\lambda_0)-1} \right\}. \tag{16}$$

Those problems of high dispersion and low diffraction efficiency explain why diffractive lenses are never used alone in systems needing low LCA. Nevertheless the lack of diffraction efficiency may be drastically diminished using multilayers [16,17] without affecting the focal distance.

5. Achromatization

In order to decrease the LCA, the combination of two lenses might prove to be very powerful ($LCA^*_{max} < 1\%$) since the lens designer may choose two wavelengths (λ_1 and λ_2) that will focus at the same point. In general, to create a doublet one uses the well-known Abbé condition given by Eq. (17) [18] in combination with the formula of the effective focal length (Eq. (18)).

$$f_1 v_1 + f_2 v_2 = 0, \tag{17}$$

$$f_{eff}^{-1} = f_1^{-1} + f_2^{-1}. \tag{18}$$

We have thus two possibilities: combining a diverging and a converging refractive lens or a converging refractive lens with a converging diffractive lens. Which of those combinations gives the best results? Before answering this question, we point out that the Eq. (17) is not fully useful for someone wishing to achromatize its system at a given focal distance. Indeed, if the formula $f_{1,d} v_{1,d} + f_{2,d} v_{2,d} = 0$ is used, $f(\lambda_C)$ and $f(\lambda_F)$ will be the same but only the focal distance of λ_d is known directly. Moreover nothing proves that having the same focal distance for λ_F and λ_C gives the smallest LCA^*_{max}. Therefore, we suggest using a more straightforward formula giving directly the focal distance of two chosen wavelengths λ_1 and λ_2.

5.1 Refractive doublet

It can be shown (Appendix B) that for a given back focal length (*bfl*) – i.e. the distance from the back of the second lens to the focal point (see Fig. 7) – the focal distance of the second lens is given by Eq. (19) and (20).
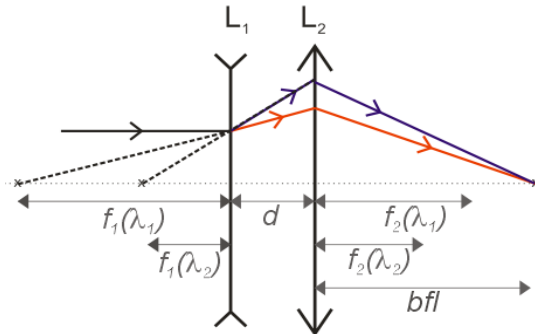

Fig. 7. Schematic representation of a doublet.

$$f_2(\lambda_1) = \frac{-B \pm \sqrt{B^2 - 4AC}}{2A}, \tag{19}$$

with

$$A = (bfl + d)\left(\frac{n_2(\lambda_1) - 1}{n_2(\lambda_2) - 1}\right)\left(1 - \frac{n_1(\lambda_2) - 1}{n_1(\lambda_1) - 1}\right),$$

$$B = bfl\left\{ d\left(\frac{n_2(\lambda_1) - 1}{n_2(\lambda_2) - 1} - \frac{n_1(\lambda_2) - 1}{n_1(\lambda_1) - 1}\right) + (bfl + d)\left(\frac{n_1(\lambda_2) - 1}{n_1(\lambda_1) - 1}\frac{n_2(\lambda_1) - 1}{n_2(\lambda_2) - 1} - 1\right)\right\}, \tag{20}$$

$$C = d\,bfl^2\left(1 - \frac{n_1(\lambda_2) - 1}{n_1(\lambda_1) - 1}\right).$$

In this equation, if $0 < d \ll bfl$, A and C are always positive while B depends on the order of the materials. The first lens will have another expression of the focal distance

$$f_1(\lambda_1) = \frac{d(bfl) - (bfl + d)f_2(\lambda_1)}{(bfl) - f_2(\lambda_1)}. \tag{21}$$

Those two equations ensure that $bfl(\lambda_1) = bfl(\lambda_2) = bfl$ where bfl, λ_1 and λ_2 are three parameters. For the other wavelengths in the refractive regime,

$$bfl_{ref}(\lambda) = \frac{f_2(\lambda)(d - f_1(\lambda))}{d - f_1(\lambda) - f_2(\lambda)}. \tag{22}$$

If the first material – of refractive index $n_1(\lambda)$ – has a dispersion higher than $n_2(\lambda)$, B will be negative and thus $f_2(\lambda)$ will be positive if the plus sign is chosen, which is in accordance with the Abbé condition (Eq. (17)). In Eq. (19), if the minus sign was chosen, then $f_2(\lambda)$ would have been negative and $f_1(\lambda)$ positive, which is not in accordance with the Abbé condition. This kind of doublets has a higher LCA than doublets obeying to Abbé conditions and may have LCA more pronounced compared with singlets. Equation (19) to (22) allow for a quicker optimisation of the LCA, when bfl is fixed we have just to find λ_1 and λ_2 optimizing the LCA. Note that the choice of bfl does not affect the *LCA** as may be understood from Eq. (6).

5.2 Hybrid lens

A hybrid lens results in the combination of a refractive and a diffractive lens. In this case, there is no need for a combination of two different optical materials since the focal length of a diffractive lens is independent of the refractive index. A hybrid lens could thus be manufactured in only one piece. Moreover the whole profile could be engraved on one surface (corresponding thus to $d = 0$), simply by summing the refractive and the diffractive profiles [19]. The focal distance of the refractive lens corresponds to one mathematical solution of a quadratic equation

$$f_{ref}(\lambda_1) = \frac{-B - \sqrt{B^2 - 4AC}}{2A} \tag{23}$$

with

$$A = (bfl + d)\left(\frac{n(\lambda_1) - 1}{n(\lambda_2) - 1}\right)\left(1 - \frac{\lambda_2}{\lambda_1}\right),$$

$$B = bfl\left\{ d\left(\frac{\lambda_2}{\lambda_1} - \frac{n(\lambda_1) - 1}{n(\lambda_2) - 1}\right) + (bfl + d)\left(\frac{\lambda_2}{\lambda_1}\frac{n(\lambda_1) - 1}{n(\lambda_2) - 1} - 1\right)\right\}, \tag{24}$$

$$C = d\,bfl^2\left(1 - \frac{\lambda_2}{\lambda_1}\right).$$

The expression of the focal distance of the diffractive lens f_{dif} given by Eq. (25) corresponds exactly to Eq. (21).

$$f_{dif}(\lambda_1) = \frac{d(bfl) - (bfl + d)f_{ref}(\lambda_1)}{(bfl) - f_{ref}(\lambda_1)}. \tag{25}$$

In the case of the hybrid lens, both f_{ref} and f_{dif} are positive for a converging lens.

6. Performance

6.1 Refractive doublet

In Table 4 the two wavelengths (λ_0 and λ_0') minimizing the $|LCA_{max}|$ have been determined with a precision of 1nm for each. For every combination of materials, under the two wavelengths of better achromatization, $|LCA_{max}|$ is presented followed by radii of curvature of the PC and the PMMA respectively. All those combinations are graphically represented in Fig. 8: each of the four PCs in combination with all PMMAs is presented. Combining a weakly crown OP (PMMA) with a flint OP (PC) may lead to very different performances. But low LCA may also be achieved with two PMMAs or two PCs. However – as it might be understood from the Abbé condition – this leads to very small radii of curvature. And since $|LCA*_{max}|$ is greater than 1% we no longer have to consider this possibility hereafter.

Table 4. Combination of PCs and PMMAs for Achromatic Doublets

OPs in PMMA	OPs in PC				Best C_{max} (line)
	PC #1	PC #2	PC #3	PC #4	
PMMA #1	1.221 (386 – 711) -114.798, 32.496	0.421 (406 – 1033) -56.380, 24.081	0.570 (402 – 1087) -41.403, 20.810	0.544 (400 – 1063) -49.691, 23.139	56,420
PMMA #2	1.260 (386 – 641) -106.638, 31.301	0.344 (400 – 693) -51.363, 22.659	0.501 (396 – 745) -37.449, 19.378	0.483 (396 – 739) -45.221, 21.723	84,505
PMMA #3	0.788 (386 – 551) -137.950, 34.087	0.124 (432 – 1107) -74.049, 27.091	0.084 (456 – 943) -55.978, 24.196	0.068 (468 – 961) -64.669, 26.059	2,137,410
PMMA #4	1.571 (387 – 806) -94.770, 30.176	0.792 (408 – 1157) -42.459, 20.537	1.081 (404 – 1175) -29.644, 16.860	0.978 (402 – 1159) -37.011, 19.498	15,942
Best C_{max} (column)	16,105	650,360	1,417,233	2,137,410	

LCA_{max} [%] (λ_0 [nm] – λ'_0 [nm]), RoC_{eq}(PC), RoC_{eq} (PMMA)

Best result of achromatization is achieved with a combination of PMMA #3 and PC #4, leading to a $LCA*_{max}$ of 0.068 corresponding to a maximal concentration of 2.1×10^6 with incoming flux at normal incidence.
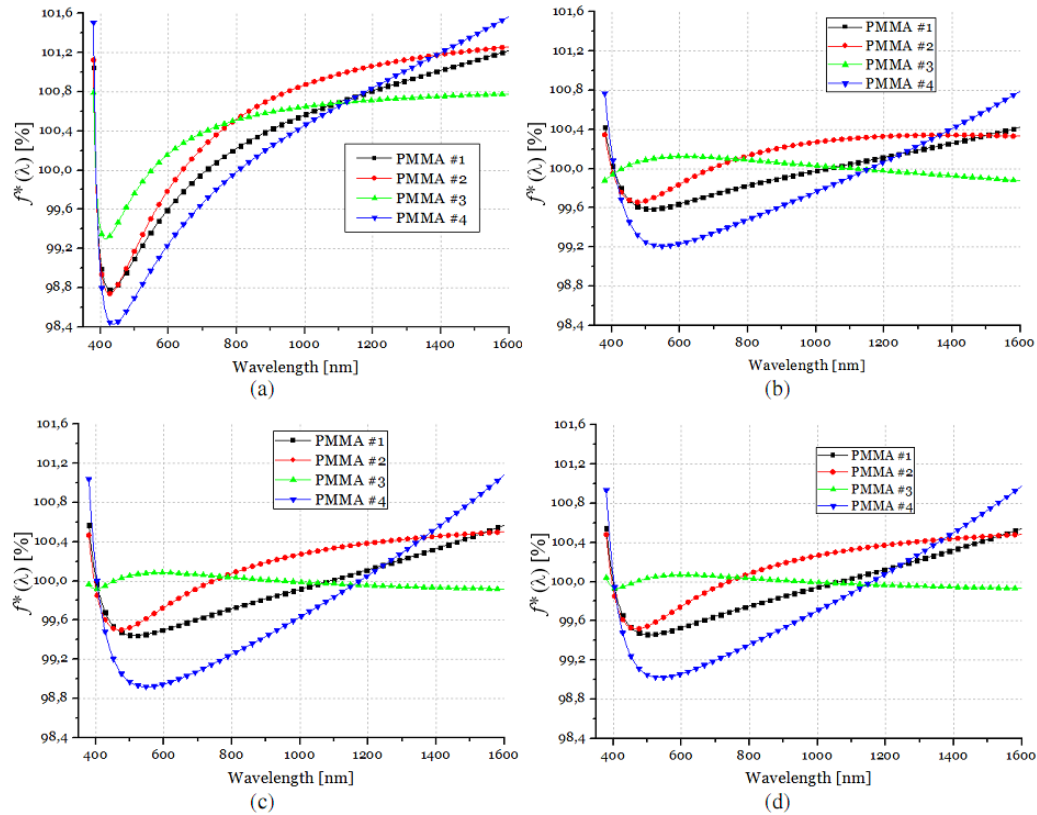
Fig. 8. Doublets with PC #1 (a), PC #2 (b), PC #3 (c) and PC #4 (d).

6.2 Hybrid lens

Since the focal distance of the hybrid lens depends only on the dispersion curve of the refractive part and on the two wavelengths of achromatization, all OPs have been considered in a single plot (Fig. 9).
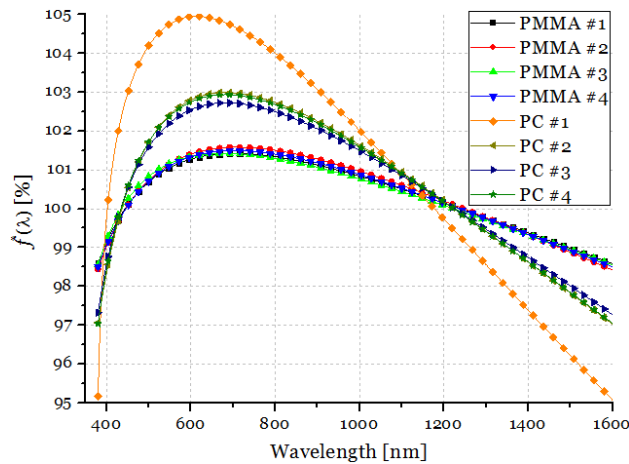

Fig. 9. Evolution of the focal distance for hybrid lenses in OP considering the curve minimizing the LCA.

Table 5 presents the two wavelengths of achromatization (λ_0 and λ'_0) giving the smallest and the equivalent radius of curvature.

Table 5. Data for achromatized hybrid lenses

OP	λ_0 and λ'_0 [nm]	RoC^*_{eq} [%]	LCA^* [%]	C^{max}_{opt}
PMMA #1	444 – 1239	51.302	1.423	4938
PMMA #2	446 – 1247	50.756	1.581	4000
PMMA #3	436 – 1223	50.409	1.450	4756
PMMA #4	446 – 1236	51.365	1.502	4432
PC #1	402 – 1177	66.775	4.954	407
PC #2	436 – 1225	63.752	2.992	1117
PC #3	434 – 1225	60.689	2.731	1341
PC #4	434 – 1223	60.466	2.965	1138

7. Discussion

This section shows the performance of achromatization for both hybrid and doublet lenses. Table 6 collects most important data to be compared.

Table 6. Major data about singlets, doublets and hybrid lenses

OPs	v_d	$v_\odot$	C^{max}_{opt} for singlets [%]	C^{max}_{opt} for hybrid [%]	Highest C^{max}_{opt} with a doublet [%]
PMMA #1	57.231	15.561	1002	4938	56,420
PMMA #2	52.270	14.868	928	4000	84,505
PMMA #3	66.522	17.990	1351	4756	2,137,410
PMMA #4	51.710	13.642	781	4432	15,942
PC #1	27.928	5.249	129	407	16,105
PC #2	29.894	7.806	270	1117	650,360
PC #3	33.746	8.854	344	1341	1,417,233
PC #4	33.271	8.106	290	1138	2,137,410

Though $v_\odot$ is in direct relation with $|LCA^*_{max}|$ of the singlet and materials with high $v_\odot$ are more suitable to be used in a hybrid lens, there is absolutely no direct relation between Abbé numbers and good achromatization with a refractive doublet. But it clearly appears that even if hybrid lenses have a smaller LCA than singlets, a refractive doublet is even more powerful decreasing the $|LCA^*_{max}|$ of the singlet up to a factor 2×10^6 while this factor is limited to $5000 \times$ in the case of hybrid lenses. Hybrid lenses have some advantages: they could be manufactured in only one material and have a higher radius of curvature. Moreover studies are still under way to improve hybrid lenses for high concentration systems [17] but at this time, lens designers would probably prefer refractive doublets to avoid the lack of diffraction efficiency and to get a higher achromatization performance.

Note that the maximum concentration is limited by the diffraction limit. For a circular lens with a radius of 10 cm and a focal of 20 cm, the concentration is limited to about 1.5×10^{16}.

8. Conclusions

Abbé formula is useful to achromatize at two wavelengths and to see that is preferable to choose two materials with Abbé numbers strongly different from each other in order to get high radii of curvature. But firstly the Abbé does not give any information about the quality of the achromatization. Secondly it does not allow choosing the focal distances of the two achromatized wavelengths. And thirdly this formula does not take into account the distance between the two lenses. Equations (19) to (22) are thus more useful for lens designers.

Not only is the Abbé number not sufficient but also the dispersion curves in the literature are limited to a spectral bandwidth and are dependent on the type of plastic, production conditions etc.

Hybrid lenses allow for fast converging systems since both lenses are converging. Unfortunately they suffer from a lack of diffraction efficiency at the focus due to spurious orders but they reduce the $|LCA^*_{max}|$ by about a factor 4.2 compared to the singlets. The maximum geometrical concentration achieved with a hybrid lens corresponds to about 5000 under normal incidence, which lies well under the maximum theoretical concentration of 46,000 under solar angular incidence.

As for refractive doublets, they allow – at normal incidence – a theoretical concentration ratio up to 50 times higher than 46,000. The linear chromatic aberration of such doublets can thus be regarded as not limiting the concentration ration. Doublets are thus good candidates to achieved very high concentration at low cost.

Appendix A

Considering a lens of diameter *2r* and a given *LCA** around $f(\lambda_0)$.
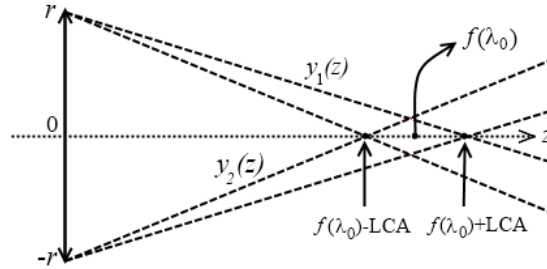

Fig. 10. Schematic representation of a converging lens with LCA.

Referring to Fig. 10, the best position of the detector is given by the intersection of the lines given by Eq. (26) and (27).

$$y_1(z) = \frac{-r}{f(\lambda_0)(1+LCA^*)}z + r, \tag{26}$$

$$y_2(z) = \frac{r}{f(\lambda_0)(1-LCA^*)}z - r. \tag{27}$$

Thus

$$\frac{1}{f(\lambda_0)(1-LCA^*)}z - 1 = \frac{-1}{f(\lambda_0)(1+LCA^*)}z + 1, \tag{28}$$

$$z\left(\frac{1+LCA^* + 1 - LCA^*}{1-\left(LCA^*\right)^2}\right) = 2f(\lambda_0), \tag{29}$$

$$z = f(\lambda_0)\left(1 - LCA^{*2}\right). \tag{30}$$

Quod erat demonstrandum.

Appendix B

The notation of this appendix follows Hecht's books [7] with the thin lens formula given by

$$\frac{1}{f} = \frac{1}{s_o} + \frac{1}{s_i}, \qquad (31)$$

where f is the focal distance, s_o the lens-object distance and s_i the lens image distance. In order to calculate the *bfl*, let's define $\hat{f}$.

$$\hat{f} = bfl + d. \qquad (32)$$

For a doublet, it doesn't matter if the first lens is the converging one or the diverging one as will be proved in the following subsections.

a) Diverging lens first

If the light coming from infinity strikes the diverging lens first, the image of the first lens – having a focal distance $f_1(\lambda)$ and a refractive index $n_1(\lambda)$ – is virtual

$$\frac{1}{f_1} = \frac{1}{s_{i1}} \qquad with\ f_1 < 0. \qquad (33)$$

The image of the first lens becomes the object of the second lens (the converging one) having a focal distance $f_2(\lambda)$ and a refractive index $n_2(\lambda)$:

$$s_{o2} = |f_1| + d. \qquad (34)$$

The final image is thus situated at a distance s_{i2} from the second lens

$$\frac{1}{s_{i2}} = \frac{1}{f_2} - \frac{1}{s_{o2}} = \frac{1}{f_2} - \frac{1}{d - f_1} = \frac{d - f_1 - f_2}{f_2(d - f_1)}. \qquad (35)$$

Thus, from the first lens, the final image is situated at

$$\hat{f} = s_{i2} + d = \frac{f_2(d - f_1)}{d - f_1 - f_2} + d. \qquad (36)$$

b) Converging lens first

Equation (33) to (36) become now

$$\frac{1}{f_1} = \frac{1}{s_{i1}} \qquad with\ f_1 > 0, \qquad (37)$$

$$s_{o2} = f_1 - d, \qquad (38)$$

$$\frac{1}{s_{i2}} = \frac{1}{f_2} - \frac{1}{s_{o2}} = \frac{1}{f_2} + \frac{1}{f_1 - d}, \qquad (39)$$

$$\hat{f} = s_{i2} + d = \frac{f_2(d - f_1)}{d - f_1 - f_2} + d, \qquad (40)$$

which is exactly the same expression as Eq. (36).

c) Expression of the focal distances

Since focal distances f_1 and f_2 depend on the wavelength, *bfl* depends on the wavelength and thus *f** also. But we would like to have the same back focal distance for two chosen wavelengths λ_1 and λ_2: $bfl(\lambda_1) = bfl(\lambda_2) = bfl$ which is equivalent to

$$\hat{f}(\lambda_1) = \hat{f}(\lambda_2) = \hat{f}. \qquad (41)$$

To ensure Eq. (41), let's determine the focal distances $f_1(\lambda)$ and $f_2(\lambda)$. Considering both lenses as thin lenses the focal distance is given by Eq. (11). Thus

$$f_1(\lambda_1) = f_1(\lambda_2)\left(\frac{n_1(\lambda_2)-1}{n_1(\lambda_1)-1}\right) = \alpha\, f_1(\lambda_2), \tag{42}$$

$$f_2(\lambda_2) = f_2(\lambda_1)\left(\frac{n_2(\lambda_1)-1}{n_2(\lambda_2)-1}\right) = \beta\, f_2(\lambda_1). \tag{43}$$

In order to facilitate the reading, we define

$$f_{ij} \triangleq f_i(\lambda_j) \tag{44}$$

from Eq. (36)

$$f_{11} = \frac{\hat{f}\, f_{21} - bfl\, d}{f_{21} - bfl} = \alpha\frac{\hat{f}\beta f_{21} - bfl\, d}{\beta f_{21} - bfl}, \tag{45}$$

effectuating the cross product

$$\left(\hat{f}\, f_{21} - bfl\, d\right)\left(\beta f_{21} - bfl\right) = \left(f_{21} - bfl\right)\alpha\left(\hat{f}\beta f_{21} - bfl\, d\right), \tag{46}$$

and separating the terms in $f_{21}^{\,2}, f_{21}, f_{21}^{\,0}$

$$f_{21}^{2}\left\{\hat{f}\beta - \hat{f}\alpha\beta\right\} + f_{21}\left\{bfl\left(\alpha d + \hat{f}\alpha\beta - \hat{f} - \beta d\right)\right\} + \left\{d\, bfl^2 - \alpha bfl^2 d\right\} = 0. \tag{47}$$

Thus

$$f_{21}\frac{-B \pm \sqrt{B^2 - 4AC}}{2A}, \tag{48}$$

with

$$\begin{cases} A = (bfl + d)\beta(1-\alpha), \\ B = bfl\left(d(\alpha-\beta) + (bfl+d)(\alpha\beta-1)\right), \\ C = d\, bfl^2(1-\alpha). \end{cases} \tag{49}$$

Finally, replacing α and β with Eq. (42) and (43), Eq. (49) turns into Eq. (24).
Quod erat demonstrandum.

Acknowledgements